DOI: 10.36108/ujees/2202.40.0191
UNIOSUN Journal of Engineering and Environmental Sciences. Vol. 4 No. 1. March. 2022

Design and Simulation of Synthetic Palm Vein Image Generation

Adebayo, O.Y., Falohun, A.S., Omidiora, E.O., Olabiyisi, S.O. and Abiona, A.K.

Abstract: The unavailability of large-scale palm vein databases due to their intrusiveness have posed challenges in exploring this technology for large-scale applications. Hence, this research modelled and generated synthetic palm vein images from only a couple of initial samples using statistical features. Variations were introduced to the three optimized statistical features (S3; mean vectors, covariance matrices and correlation coefficient, S2; mean vectors and covariance matrices, S1; mean vectors, NS; acquired images) which were used to generate synthetic palm vein images employing Self Organizing Map (SOM) as classifier and were evaluated based on Equal Error Rate (EER), Average Recognition Accuracy (ARA) and Average Recognition Time (ART). The results obtained from the experiment showed that EERs were 0.22, 0.51, 0.58 and 4.36 for S3, S2, S1 and NS respectively. S3 had superior ARA (99.83%) compared with S2 (99.77 %), S1 (99.70 %) and NS (98.33 %). The ARTs obtained were 84.97s, 75.55s, 84.04s and 681.74s for S1, S2, S3 and NS respectively with S2 (75.55s) having significantly least value. This is on the ground that the more the optimized statistical features, the better the recognition accuracy. The research outcome justifies the extraction of mean vectors, covariance matrices and correlation coefficient with *GA-SOM*.

Keywords: Palm vein, Mean, Covariance, Correlation coefficient

I. Introduction

Large-scale biometric databases that include enough samples for training and testing are required for authentication systems. Most of the evaluations are based on a limited database since there are no public palm vein databases with sufficient samples. However, it is challenging to get palm vein images because they are highly intrusive [1], and it takes time and cooperation of subjects to gather sufficient palm vein data. Likely mitigation to these problems is working with synthetic biometrics.

Adebayo, O.Y. (Department of Information and Communication Technology, Osun State University, Osogbo, Osun-State, Nigeria)
Falohun, A.S., Omidiora, E.O. and Olabiyisi, S.O. (Department of Information and Communication Technology, Ladoke Akintola University of Technology, Ogbomosho, Oyo-State, Nigeria)
Abiona, A.K. (Department of Information and Communication Technology, Federal Polytechnic, Ile Oluji, Ondo-State, Nigeria)
Corresponding author: olajide.adebayo@uniosun.edu.ng
Telephone Number: +2348035234019
Submitted: 01-02-2022
Accepted: 25-03-2022

A method for synthetic fingerprint image generation using a mathematical model was developed by [2]. The randomly produced synthetic images have a limited number of parameters supplied to them. Acquisition devices produced an exceptional amount of variations, and Synthetic Fingerprint Generation (SFinGe) employed these to create a succession of prosthetic fingers, all with the same fingerprint. Synthetic fingerprints created from the method had a remarkable resemblance to genuine fingerprints, which was subsequently employed in fingerprint-based systems for performance evaluation. Realistic sensor-dependent backdrops were not included in the development of the ad-hoc stage.

[3] proposed a novel recognition algorithm based on subspace-mapping for heterogeneous face recognition and synthesis. The method takes Canonical Correlation Analysis (CCA) subspace as a medium to match the heterogeneous images, and further

improve the recognition accuracy. Local Binary Pattern (LBP) was used as facial representation for near infrared, visual light and 3D range images. Then CCA was applied to learn the mapping between different face patterns. The algorithm depends on the linear mapping between the images, the preprocessing is crucial and the pixel alignment will significantly affect the experimental results.

Hybrid Principal Component Analysis (PCA) and Self-Organizing Map (SOM) were used in a palm vein authentication system developed [4]. The unscaled (between 0 and 255) and scaled (between 0 and 0.9) scales were evaluated. Image resolutions, training datasets, recognition time, and accuracy were used as performance metrics. A feasible technique was found in a current biometric application to be put into practice. Further investigation on the effectiveness of a strategy to identify the most discriminating information in the palm vein was suggested.

[5] developed an approach for modifying synthetic fingerprints. Warts and atopic dermatitis are two skin illnesses considered. Black spots were used for warts while lines and coloured were used for eczema. Depending on the produced wart size, warts datasets saw a drop in matching scores when tested with the VeriFinger algorithm. Fingerprints afflicted by eczema exhibited a drop in matching scores. When datasets created with patches enabled were compared to a control group, the matching score declined to 68.2% of the control group score. The matching score dropped to 64.30% when patches and eczema lines were merged. An additional goal for the future is to look at the relationships between skin disease characteristics and joint-feature models to determine whether they are required.

[6] proposed an algorithm for creating highly realistic synthetic datasets of pedestrians in a walkway as a substitute for real images. The synthetic images were fed to a designed Deep Convolutional Neural Network (DLCNN) to learn from. The result revealed that incorporation of synthetic data as a well-suited surrogate or missing real along with alleviating required exhaustive labelling.

The work of [7] leveraged facial parts locations for better attribute prediction; a facial abstraction image that contained both local facial parts and facial texture information. Extensive evaluations conducted showed that state of the art performance was achieved. Future work will include integrating variations resulting from a change in viewing conditions. This will require rendering facial appearances using a face 3D model.

[8] develop a controllable text-to-image using a method called Control General Adversarial Network (controlGAN). This was achieved using word-level spatial and channel-wise attention-driven generator. They proposed a word-level discriminator to provide fine-grained supervisory feedback by collecting words with image region, facilitating training an effective generator that is able to manipulate specific visual attributes. Experimental results revealed the proposed method outperformed the existing method in natural language description.

[9] observed that images captured of football players during a football match had low resolution even when cameras are of high resolution. They proposed an approach to resolve issues posed by low-resolution images. A simple Python script for the synthetic image was created instead of manual annotations. The raw synthetic images were transformed into a more realistic image using Vanilla Cycle Generative Adversarial Network (CGAN) and trained using Cascade Pyramid Network

(CPN) model. They were able to achieve similar precision with their images as the one of CPN model trained with Common Object in Context (COCO).

[10] evaluated the feasibility of a deep learning method for fast reconstruction of synthetic Magnetic Resonance Imaging (MRI). Forty-four subjects were used for training and fourteen for testing the model. Multiple dynamic multi-echo sequences (MDME), Quantification maps and the magic software were employed for image acquisition, weighing and creation. A small error exists between generated and reference images. The study validated the deep learning method as a superior method for synthetic image generation.

Several synthetic databases have been developed [face, fingerprint, iris, handwriting and signature] however, synthetic palm vein image generation has not at present fulfilled its undoubted potential. Hence, the aim of the study was to model and generate synthetic palm vein images from only a couple of initial samples by introducing variations to the statistical features (mean, covariance and correlation coefficient) employing statistical and Genetic Algorithm (GA) approaches.

II. Materials and Methods

This part presents the methodology employed in this research work. Palm vein images were acquired using M2SYS PalmSecure palm vein scanner. The second stage is the preprocessing procedure while low-cost method was used for features extraction. The features were selected and optimized by Genetic Algorithm (GA). Variation were introduced to the optimized features (S3; mean vectors, covariance matrices and correlation coefficient, S2; mean vectors and covariance matrices, S1; mean vectors, NS; acquired images) to generate synthetic palm vein images (See Figure 1).

M2SYS PalmSecure palm vein scanner was used to capture 500 palm vein images of different subjects. All these images were stored in the palm vein database and images served as training and testing datasets. The palm vein images acquired were fed as input to the preprocessing stage. The following sets of preprocessing steps necessary to improve the clarity of the vein pattern structure and localize the vein grid were an apple.

A. Palm Vein Image Normalization

The histogram of a palm vein image as proposed by [11] with gray levels in the range [0, L–1] is a discrete function $z(r) = n_r$, where r is the gray level and n_r is the number of pixels in the image having gray level *r*. Using Band Limit Histogram Equalization for palm vein image normalization as shown in Figure 2, histogram equalization is accomplished for certain intensity band between lower limit *b* and upper limit *c*. *T(r)* is cumulative distribution function in the intensity range between *b* and *c* and is given by (Eq. 1 and 2).

$$T(r) = \sum_{k=b}^{r} z(k), \quad b \le r \le c. \tag{1}$$

$$T_n(r) = T(r)/T(c) \tag{2}$$

where *T(c)* is the maximum value of the cumulative distribution function in the selected intensity band. The normalized values can be scaled between b and c (Eq. 3) as follows;

$$\bar{T}(r) = int\left[\frac{T_n(r) - T_n(b)}{1 - T_n(b)} * (c - b) + b\right], \quad b \le r \le c, \tag{3}$$

where $T_n(b)$ is the minimum value in the cumulative probability density function vector $T_n(r)$. $\bar{T}(r)$ is the transformed value for each gray level in the selected intensity band.

B. Palm Vein Image Segmentation

A Gabor function in the spatial domain is a sinusoidal modulated Gaussian. For a 2-D Gaussian curve with a spread of σ_x and σ_y in the x and y directions, respectively, and a modulating frequency of σ_0, the real impulse response of the filter is given by (Eq. 4)

$$h(x,y) = \frac{1}{2\pi\sigma_x\sigma_y} exp\left\{-\frac{1}{2}\left[\frac{x^2}{\sigma_x^2} + \frac{y^2}{\sigma_y^2}\right]\right\}.\cos(2\pi\sigma_0 x) \quad (4)$$

In the spatial-frequency domain, the Gabor filter becomes two shifted Gaussians at the location of the modulating frequency. The equation of the 2-D frequency response of the filter is given by (Eq. 5)

$$H(u,v) = exp\{-2\pi^2[\sigma_x^2(u - u_0) + \sigma_y^2 v^2\} + exp\{-2\pi^2[\sigma_x^2(u + u_0) + \sigma_y^2 v^2\} \quad (5)$$

Mean, covariance and correlation coefficient of the normalized palm vein images were extracted using the low-cost method presented in Algorithm 1.

i. Let X represent acquired palm vein with n rows and m columns. Let X' represent synthetic palm vein to be generated, with n' rows and m columns.
ii. X can be viewed as an $n \times m$ matrix and X' can be viewed as an $n' \times m$ matrix.
iii. The low-cost method presented in Algorithm 1 preserved the statistical properties of the normalized palm vein images X, in the reproduced synthetic palm vein images X'. (Eq. 6, 7 and 8).

Algorithm 1: (Low-Cost Method for Extraction of Statistical Properties

1. Generate A, which is a random $n' \times m$ matrix, such that the covariance matrix of A is the identity matrix.
2. Compute the covariance matrix C of the original data matrix X.
3. Use the Cholesky decomposition on C to obtain

$$C = U' \times U \quad (6)$$

where U is an upper triangular matrix and U' is the transposed version of U.

4. Obtain the synthetic data set X' as a matrix product:

$$X' = A.U \quad (7)$$

Note That the covariance matrix of X' equals the covariance matrix of X.

5. Due to the construction of matrix A, the mean of each variable in X' is 0. In order to preserve the mean of variables in X, a last adjustment is performed. If $\bar{x}_j$ be the mean of the j-th variable in X, then $\bar{x}_j$ is added to the j-th column (variable) of X':

$$x'_{ij} := x'_{ij} + \bar{x}_j \ for\ i = 1, \dots, n' \ and \ j = 1, \dots m \quad (8)$$

FS ensures only relevant features of the palm vein images are used in the synthetic palm vein image generation process. As depicted in Algorithm 2, GA was employed for features selection. GA initially starts with a number of solutions known as population. These solutions were represented by using string coding of fixed length. After evaluating each chromosome using fitness function and assigning a fitness value, three different operators such as mutation, selection, and crossover were used to update the population. A repetition of these three operators is known as a generation. The new chromosome replaced the chromosome with the lowest survival rate (See Figure 4).

Algorithm 2: Stepwise Procedure of the GA

1. Start
2. Get palm vein features set
3. Initialize parameters (set gen<= number of generations; set n <= population size, mutation probability)
4. Generate randomly distributed chromosomes to form initial population

5. Encode features by a chromosome {using bit strings encoding}
6. Gencount <=0
7. Rank chromosomes based on its uniqueness {first chromosome occurrence = 1, subsequent occurrence = 0
8. Arrange chromosomes based on their fitness value {Accept features with bit value = 1 and reject features with bit value = 0}
9. Mutate selected chromosomes based on mutation probability
10. Select chromosome with a best fitness value
11. Perform crossover on parent chromosomes to form new offspring and replace the weak chromosomes with the new offspring
12. Gencount <= gencount + 1 and repeat until total number of generations
13. If gencount = gen then go to 14 else 7
14. Output chromosome with the highest fitness value (features selected)

Figure 1 describes how synthetic palm vein images were generated. Mean, covariance and correlation coefficient were three statistical features introduced to derive synthetic palm vein images. Variations were introduced to generate realistic synthetic palm veins as follows:

a. S1 (Mean)
b. S2 (Mean and Covariance)
c. S3 (Mean, Covariance and Correlation Coefficient)

C. Experiments

In the first experiment, identification performances of each of S1, S2, S3 and NS (Non-Synthetic /Original images) were conducted. For S1, statistical property (mean) was used for the synthetic palm vein image generation. For S2, statistical properties (mean and covariance) were used for the synthetic palm vein image generation. Finally, S3, statistical properties (mean, covariance and correlation coefficient) were used for the synthetic palm vein image generation. In all SOM was used as a classifier for all systems considered. The flowchart shows the training and testing using SOM.

The second experiment investigated the measurement of similarities between the synthetically generated palm vein images and the original palm vein images. Synthetic palm vein images of the best in performance in the first experiment and all the original palm vein images were evaluated to determine their degree of similarities in their features. In S4, the synthetic images generated were employed as training images and the original images were used as testing images. However, in S5, the original images were employed as training images and synthetic images generated were used as testing images.

The performance of the SOM on both trained and tested S1, S2 and S3 were evaluated based on EER, FAR, FRR, ART and RA.

i. Equal Error Rate (EER): This error rate corresponds to the point at which the FAR and FRR cross (compromise between FAR and FRR). It is widely used to evaluate and to compare biometric authentication systems.
ii. Average Recognition Accuracy: this is the main measurement to describe the accuracy of a recognition system. It represents the average number of palm vein that are correctly recognized from the total number of palm vein tested.
iii. Average Recognition Time: this is the main measurement to describe the recognition time. It represents the average time it takes palm vein to be correctly recognized from the total number of palm vein tested.

$$RA = \frac{Number\ of\ correctly\ recognized\ palm\ vein}{Total\ number\ of\ palm\ vein\ tested} \quad (9)$$

III. Results and Discussion

A. Results

The results of the implementation of the synthetic palm vein generation system are presented in this section.

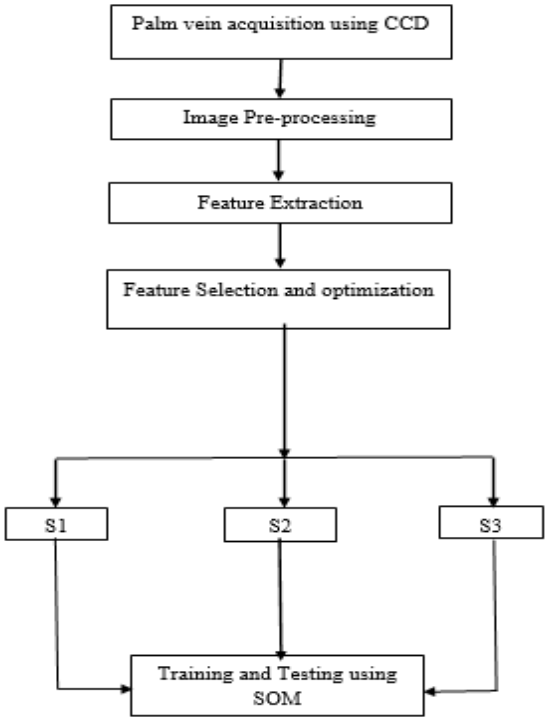

Figure 1 Block Diagram of the Developed Synthetic Palm Vein Image Generation System

B. Discussion

In Table 1, EER of the systems under consideration were 0.22, 0.51, 0.58 and 4.36 for S3, S2, S1 and NS respectively. S3 has the least EER value in all the systems under consideration, it exercised the topmost restraints to images that did not take part in the training and the least restraints to the training dataset. In view of this, it is the most secure and has the best performance because it is inbuilt with sufficient optimized statistical features.

In addition, ARA of 99.68% for S1; 99.73% for S2; 99.80% for S3; and 95.78% for Non-Synthetic. S3 had the highest ARA (99.80%) of the four systems and this is on the ground that the more the optimized statistical features

Figure 2: Flowchart showing Training and Testing using SOM

Table 1 Authentication Performance and ART of the Systems

Access Control Systems	ARA (%)	ART(*s*)	EER
NS	95.78	681.74	4.36
S1	99.68	84.97	0.58
S2	99.73	75.55	0.51
S3	99.80	84.04	0.22

Table 2: Estimated Similarity Measures for Synthetic and Acquired Images

Metric	S4 (Synthetic (Training) Original (Testing))	S5 (Synthetic (Testing) Original (Training))
EER	0.43	1.43
ARA (%)	99.00	97.50
ART (s)	12.13	680.13

that were included in training and testing, the better recognition accuracy. This is an indication that optimized statistical features (which are the mean, covariance and the correlation coefficient) with respect to the developed systems contributed significantly to the overall performance as access control systems and/or identification systems. ART obtained for the systems are 84.97s, 75.55, 84.04s and 681.74s for S1, S2, S3 and NS respectively, with S2 (75.55s) having significantly least value. This implied that the average rate of certifying the identity of an individual is significantly the least with respect to S2.

The second experiments were performed in order to measure the level of similarities of synthesized palm vein images with acquired original palm vein images, Table 2 showed the ARA of the two test sets of images with 99.00% for S4 (Synthetic images (training) and Original images (testing)) and 97.50% for the S5 (Original images (training) and Synthetic images (testing)). ART obtained for the images are 12.13s and 680.13s for S4 and S5 respectively. In addition, the EER was 0.43 for S4 and 1.43 for S5. This implies that S4 have the best access control performance, the least time for certifying the identity of an individual and the highest restraint to images that did not partake in training. Also, the original images employed in testing the system have enough statistical properties to match the training images which have only three statistical properties as indicated in Figure 5.

Consequently, in the first experiment, the validation of the performance of synthetic samples with respect to S1, S2, and S3 and the acquired sample images justifies the fact that the extraction of mean, covariance and correlation coefficient from the acquired palm vein images with *GA-SOM* as classifier significantly outperformed acquired palm vein. Moreover, in the second experiment, S4 (Synthetic (training samples) Original (testing samples) was found to be significantly better in performance than S5 (Original (training samples and Synthetic (testing samples)). The main reason for S4 significant performance (with respect to all the metrics used) over S5 could be attributed to the fact that each of the original images used as a test sample inherently has all the statistical properties to match the synthetic palm vein images (which only contains three statistical properties) used in training. This confirmed that statistically synthetic images once generated, can be populated efficiently enough to serve as the train sample while the original palm vein images can be employed as the test sample.

IV. Conclusion

Convincingly, an indication of optimized statistical features contributed significantly to the overall performance of synthetic palm vein image generation. Also, this confirmed that statistically synthetic images once generated, can be populated efficiently enough to serve as train samples while the original palm vein images can be employed as the test sample.

Figure 3: Samples of Acquired Palm Vein Images

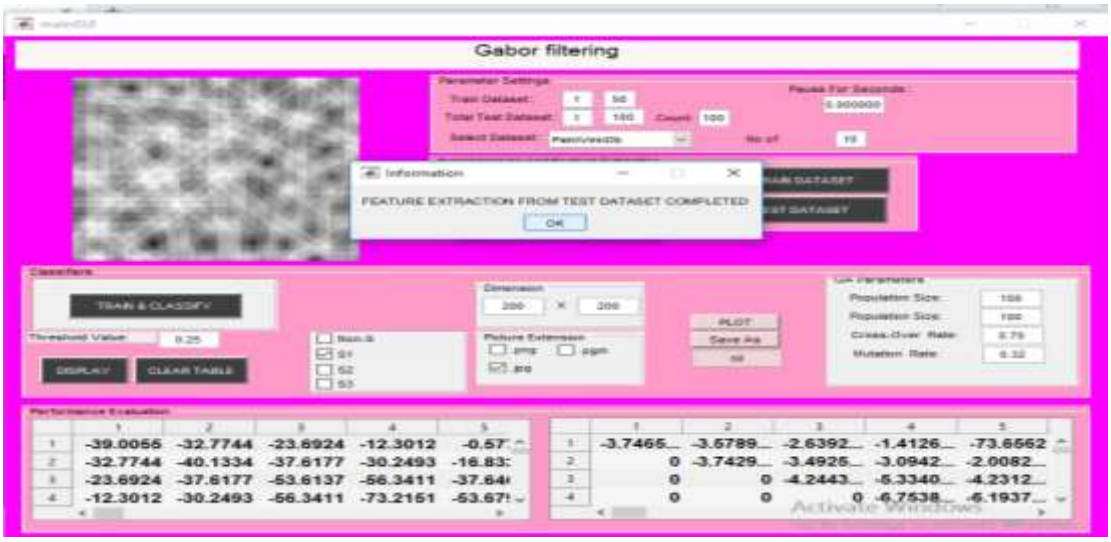

Figure 4: Samples of Feature Extracted from Palm Vein Images

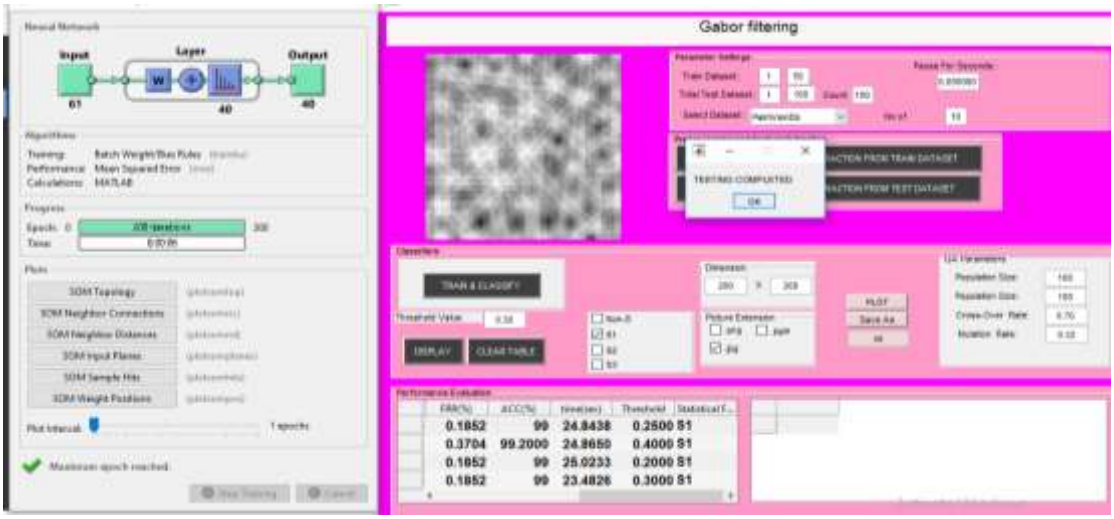

Figure 5: Graphical User Interface of Classification stage

Conclusively, the work has presented a method to create a synthetic palm vein database, which is reasonable facsimiles of real palm vein images

References

[1] Lee, Y.P. "Palm Vein Recognition Based on a Modified (2D)2LDA", *Journal of Signal, Image and Video Processing*, vol. 9, no. 1, 2013, pp. 229–242.

[2] Cappelli, R., Maio, D. and Maltoni, D. "Synthetic Fingerprint-Database Generation", *16th International Conference on Pattern Recognition*. Québec City, 2002, pp. 744-747.

[3] Mengyi, L., Zhiyong, Y., Yufeng, M., Xingwei, C. and Qian, Y. "Heterogeneous Face Recognition and Synthesis Using Canonical Correlation Analysis", *Journal of Conv. Information Technology,* vol. 7, no. 8, 2012, pp. 398- 407.

[4] Omidiora, E.O., Oladosu, J.B., Ismaila, W.O., Agbaje, K.M. and Adeniyi, A.Y. "Palm Vein Recognition System Using Hybrid Principal Component Analysis and Artificial Neural Network", *International Journal of Advance Research in Computer Science and Software Engineering*. vol. 3, no. 7, 2013, pp. 69-78.

[5] Milan, B. and Martin, D. "Generation of Skin Diseases into Synthetic Fingerprints", *International Journal of Image Processing*, vol. 10, no. 5, 2016, pp. 229-248.

[6] Hadi, K., Ekbatani, O., Pujol and Santi, S. "Synthetic Data Generation for Deep Learning in Counting Pedestrians", 6th *International Conference on*

Pattern Recognition Applications and Methods, 2017, pp. 318-323.

[7] Keke, H., Yanwei, F., Wuhao, Z., Chengjie, W., Yu-Gang, J., Feiyue, H. and Xiangyang, X. "Harnessing Synthesized Abstraction Images to Improve Facial Attribute Recognition", *Proceedings of the Twenty-Seventh International Joint Conference on Artificial Intelligence*, 2018, pp. 733- 740.

[8] Bowen, L., Xiaojuan, Q., Thomas, L. and Philip, H.S. "Controllable Text-to-Image Generation", *33rd Conference on Neural Information Processing Systems*, 2019, Vancouver, Canada, pp. 1-11.

[9] Michal, S., Grzegorz, S. and Tomasz, T. "Synthetic Image Translation for Football Players Pose Estimation", *Journal of Universal Computer Science*, vol. 25, no. 6, 2019, pp. 683-700.

[10] Yawen, L., Haijun, N., Pengling, R., Jialiang, R., Xuan, W., Wenjuan, L., Heyu, D., Jing, L., Jingjing, X., Tingting, Z., Han, L., Hongxia, Y. and Zhenchang, W. "Generation of Quantification Maps and Weighted Images from Synthetic Magnetic Resonance Imaging using Deep Learning Network.

[11] Mohammed, S.S., Nabila, E., Fathi, F. and Ghada, K.G. "Band-Limited Histogram Equalization for Mammograms Contrast Enhancement", *International Biomedical Engineering Conference*, Cairo, Giza, 2012, pp. 154-15.

[12] Jumanal, S. and Holi, G. "On-line Handwriting English Character Recognition Using Genetic Algorithm", *International Journal of Computer Trends and Technology*, vol. 4, no. 6, 2013, pp. 1885-1890.